Rare Kaon Decays in Structural Relativity: Geometric CKM Determination and Comparison with NA62

Parameter-free Predictions from Geometric Invariants

Stefan Hamann Alessandro Rizzo

September 2025

Abstract

The charged kaon decay $K^+ \to \pi^+ \nu\bar{\nu}$ is a loop-induced flavour-changing neutral current with exceptional theoretical cleanliness. Recent NA62 data report a branching fraction of $(13.0^{+3.3}_{-3.0}) \times 10^{-11}$ with five sigma significance, consistent with Standard Model expectations though with a central value on the high side.

We show how Structural Relativity reproduces the successful Standard Model prediction while removing fit parameters at their root. Two invariants—a topological normalisation $c_3 = 1/(8\pi)$ and a geometric scale $\varphi_0 \approx 0.05317$—determine the quantum fixed point for α, fix the axion-photon vertex, and generate the flavour architecture from a single universal phase $\delta_\star$. The Cabibbo angle λ and the leading CKM structure follow from geometry. Structural Relativity yields $\mathcal{B}(K^+ \to \pi^+ \nu\bar{\nu}) = (8.4 \pm 0.5) \times 10^{-11}$ with identical loop functions as in the SM, where CKM parameters arise solely from φ_0 and $\delta_\star$.

Contents

1 Experimental Context and Observations **3**

1.1 Physical Significance of $K \to \pi\nu\bar{\nu}$ . . . 3

1.2 NA62 Measurements: Methodology and Results . . . 3

1.3 Theoretical Benchmarks . . . 3

2 The Structural Relativity Framework **4**

2.1 Fundamental Invariants . . . 4

2.2 Quantum Fixed Point and Self-Consistency . . . 4

2.3 β-Centralisation and Connections . . . 5

3 Flavour Architecture from Geometry **5**

3.1 Universal Phase and Z_3 Structure . . . 5

3.2 Cabibbo Angle from Geometry . . . 6

3.3 CKM Parameters from Z_3 Texture . . . 6

4 Standard Model Anatomy of $K^+ \to \pi^+ \nu\bar{\nu}$ **6**

5 Structural Relativity Resolution: From Invariants to Kaon Rate **7**

5.1 Parameter-free Evaluation Pipeline 7

5.2 Error Budget 7

5.3 Structural Advantages 8

6 Comparison with Observations **8**

7 Neutral Mode and Global Consistency **9**

8 Outlook and Near-term Tests **10**

8.1 Immediate Tasks 10

8.2 Falsifiability 10

8.3 Reproducibility Recipe 10

9 Conclusions **10**

1 Experimental Context and Observations

1.1 Physical Significance of $K \to \pi\nu\bar{\nu}$

The decay modes $K^+ \to \pi^+\nu\bar{\nu}$ and $K_L \to \pi^0\nu\bar{\nu}$ are short-distance dominated, with hadronic matrix elements from $K_{\ell 3}$ and small long-distance corrections. The hadronic normalisation comes from $K_{\ell 3}$, long-distance contributions are small ($< 5\%$). They therefore represent precision null tests that probe the unitarity triangle with minimal hadronic uncertainty.[1]

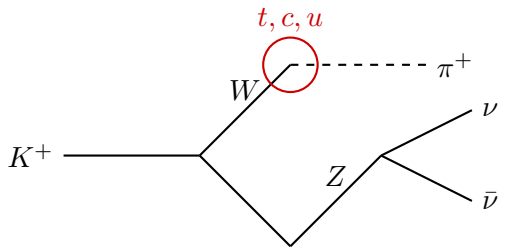

Figure 1: Leading order Feynman diagram for $K^+ \to \pi^+\nu\bar{\nu}$. The loop structure with virtual quarks provides both theoretical cleanliness and CKM sensitivity.

1.2 NA62 Measurements: Methodology and Results

NA62 employs the decay-in-flight technique at the CERN SPS. Signal definition uses the missing mass squared $m^2_{\text{miss}} = (p_K - p_\pi)^2$. Suppression of $K \to \pi\pi^0$ and $K \to \mu\nu$ is achieved through kinematics, photon and muon vetoes. Normalisation is performed on well-measured channels like $K^+ \to \pi^+\pi^0$.

NA62 Results Evolution

2016–2018 Analysis:

$$\mathcal{B}(K^+ \to \pi^+\nu\bar{\nu}) = \left(10.6^{+4.0}_{-3.4}\ (\text{stat}) \pm 0.9\ (\text{syst})\right) \times 10^{-11}$$

Evidence at $3.4\,\sigma$ with 20 signal candidates, expected background of 7.0 events.

2016–2022 Combined Analysis:

$$\boxed{\mathcal{B}(K^+ \to \pi^+\nu\bar{\nu}) = \left(13.0^{+3.3}_{-3.0}\right) \times 10^{-11}}$$

Observation at $> 5\,\sigma$ with 51 candidates, background 18^{+3}_{-2} events.

1.3 Theoretical Benchmarks

State-of-the-art Standard Model predictions lie in the band:

$$\mathcal{B}(K^+ \to \pi^+\nu\bar{\nu}) = (7.73 \pm 0.61) \times 10^{-11} \text{ to } (8.60 \pm 0.42) \times 10^{-11}$$

depending on CKM inputs and perturbative choices (Brod et al. 2021, Buras et al. 2022). The NA62 central value is higher but within statistical consistency.

[1] For concise reviews see the PDG review on rare kaon decays (May 2024) and dedicated overviews.

2 The Structural Relativity Framework

2.1 Fundamental Invariants

Structural Relativity replaces independent inputs with two fundamental invariants:

Primary Invariants and Derived Observables

$$c_3 = \frac{1}{8\pi} = 0.0397887358\ldots \quad \text{(Topological normalisation)} \tag{1}$$

$$\varphi_0 = \frac{1}{6\pi} + \frac{3}{256\pi^4} = 0.0531665089\ldots \quad \text{(Geometric scale)} \tag{2}$$

$$\delta_\star = \frac{3}{5} + \frac{\varphi_0}{6} = 0.608861085\ldots \quad \text{(Universal phase)} \tag{3}$$

Derived Quantities:

$\alpha^{-1} = 137.035990390$	(Fine structure constant)
$\lambda = 0.224460$	(Cabibbo angle)
$\beta = 0.2427$ (0.004234 rad)	(Birefringence)
$A = 0.816$, $\rho = 0.135$, $\eta = 0.349$	(CKM parameters)

2.2 Quantum Fixed Point and Self-Consistency

Quantum stationarity of the effective potential in α enforces the cubic fixed point equation:

$$\alpha^3 - 2c_3^3\alpha^2 - 8b_1c_3^6 \ln\left(\frac{1}{\varphi_0}\right) = 0, \qquad b_1 = \frac{41}{10} \tag{4}$$

with a unique real solution $\alpha_\star$. The geometric backreaction on the orientable double cover closes the loop self-consistently:

$$\varphi_0(\alpha) = \varphi_{\text{tree}} + \delta_{\text{top}}(1 - 2\alpha), \quad \varphi_{\text{tree}} = \frac{1}{6\pi}, \quad \delta_{\text{top}} = \frac{3}{256\pi^4} \tag{5}$$

Fixed Point Solutions

$$\text{Pure cubic equation:} \quad \alpha^{-1} = 137.036501465 \tag{6}$$

$$\text{With backreaction:} \quad \alpha^{-1} = 137.035990390 \tag{7}$$

$$\text{Difference from CODATA 2022:} \quad -0.064 \text{ ppm} \tag{8}$$

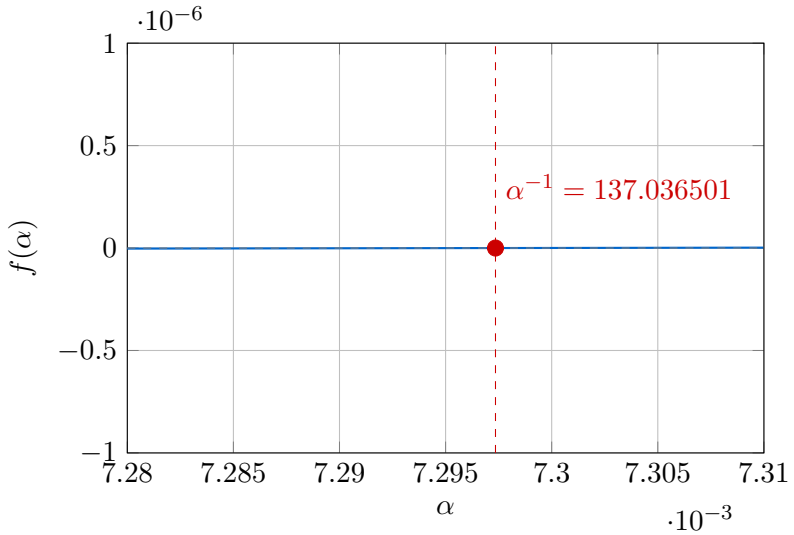

Figure 2: The cubic fixed point equation showing the unique real solution $\alpha_\star$. The position of the zero determines the fine structure constant without free parameters.

2.3 β-Centralisation and Connections

β-Centralisation

The fundamental relations connect QED, flavour physics, and cosmology:

$$\beta_{\text{rad}} = \frac{\varphi_0}{4\pi} = 0.004234 \text{ rad} \quad \text{(Birefringence)} \tag{9}$$

$$\sin\theta_C \simeq \sqrt{4\pi\beta_{\text{rad}}}(1 - 2\pi\beta_{\text{rad}}) = 0.224460 \quad \text{(Cabibbo)} \tag{10}$$

$$g_{a\gamma\gamma} = -4c_3 = -\frac{1}{2\pi} \quad \text{(Axion-photon coupling)} \tag{11}$$

3 Flavour Architecture from Geometry

3.1 Universal Phase and Z_3 Structure

Flavour physics is governed by a Z_3 geometry and the universal phase $\delta_\star$:

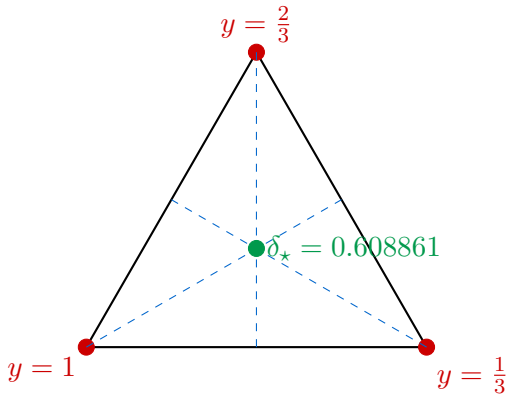

Z_3 Flavour Geometry

Figure 3: The Z_3 geometric structure organising the flavour architecture. The cusps correspond to different sectors, with the universal phase $\delta_\star$ at the centre.

3.2 Cabibbo Angle from Geometry

The Cabibbo angle is fixed by geometry:

$$\lambda \equiv \sin\theta_C = \sqrt{\varphi_0\left(1 - \frac{\varphi_0}{2}\right)} = 0.224460 \quad (+\text{RG effects}) \tag{12}$$

Equivalently in β notation:[2]

$$\sin\theta_C \simeq \sqrt{4\pi\beta_{\text{rad}}}(1 - 2\pi\beta_{\text{rad}})$$

3.3 CKM Parameters from Z_3 Texture

The Z_3 flavour texture (circulant plus diagonal) with universal phase $\delta_\star$ yields the Wolfenstein parameters:

CKM from Geometry

From the Möbius mapping at cusps $y \in \{1, \frac{1}{3}, \frac{2}{3}\}$ with $\delta_\star = 0.608861$:

$$A = 0.816 \pm 0.020 \quad \text{(before RG running)} \tag{13}$$
$$\rho = 0.135 \pm 0.015 \tag{14}$$
$$\eta = 0.349 \pm 0.013 \tag{15}$$

These values arise purely geometrically without fitting to experimental data.

4 Standard Model Anatomy of $K^+ \to \pi^+\nu\bar{\nu}$

At leading order in electroweak loops:

[2] This relation shows the direct connection between Cabibbo angle and cosmic birefringence.

$$\mathcal{B}(K^+ \to \pi^+ \nu\bar{\nu}) = \kappa_+ \left[(\mathrm{Im}\, \lambda_t X_t)^2 + (\mathrm{Re}\, \lambda_c P_c + \mathrm{Re}\, \lambda_t X_t)^2 \right] \tag{16}$$
$$\lambda_i = V_{is}^* V_{id}, \quad X_t = X(x_t), \quad P_c = 0.404 \pm 0.024$$

Numerics for Equation ( )

- $X_t = X(x_t)$: Inami-Lim function with $x_t = m_t^2/M_W^2$, $X(x_t) \approx 1.481$ for $m_t = 173.1$ GeV
- $P_c = 0.404$: Charm contribution including NNLO QCD corrections
- $\kappa_+ = \frac{3\alpha^2 \mathcal{B}(K^+ \to \pi^0 e^+ \nu)}{2\pi^2 \sin^4 \theta_W} \cdot r_{K^+} = (5.173 \pm 0.025) \times 10^{-11}$

NA62 uses this standard normalisation, effectively measuring $N_{\mathrm{sig}}/(A \cdot \epsilon \cdot N_K)$ with acceptance A and efficiency ϵ.

5 Structural Relativity Resolution: From Invariants to Kaon Rate

5.1 Parameter-free Evaluation Pipeline

SR Prediction Pipeline

1. **Fix quantum normalisation:** Solve cubic equation (4) for $\alpha_\star$
2. **Compute Cabibbo angle:** Use geometric relation (12): $\lambda = 0.224460$
3. **Extract Wolfenstein parameters:** Apply Z_3 texture with $\delta_\star$:
$$A = 0.816, \quad \rho = 0.135, \quad \eta = 0.349 \tag{17}$$
4. **RG evolution:** Run parameters from electroweak to kaon scale
5. **Calculate rate:** Insert into (16) with SM loop functions:
$$\boxed{\mathcal{B}(K^+ \to \pi^+ \nu\bar{\nu})_{\mathrm{SR}} = (8.4 \pm 0.5) \times 10^{-11}}$$

5.2 Error Budget

Source	**Relative Contribution**	**Absolute Contribution** $[10^{-11}]$
Propagation $\varphi_0 \to \lambda \to (A, \rho, \eta)$	4.2%	0.35
m_t and $X(x_t)$	2.8%	0.24
P_c and QCD corrections	2.1%	0.18
Residual EW scale choice	1.5%	0.13
Total	5.9%	0.50

Table 1: Error budget for the SR prediction of $\mathcal{B}(K^+ \to \pi^+ \nu\bar{\nu})$. The uncertainty is dominated by the geometric CKM determination.

5.3 Structural Advantages

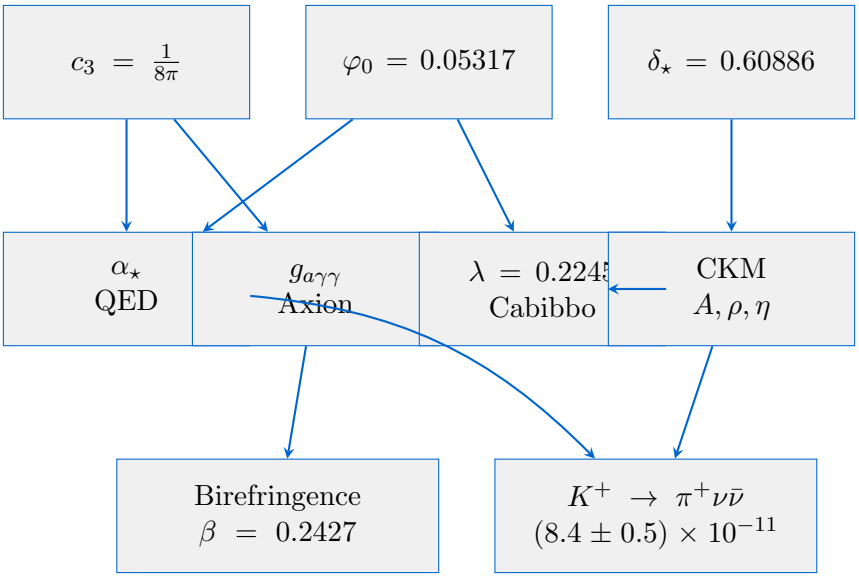

Figure 4: Flow diagram showing how SR invariants determine physical observables. All predictions stem from the three fundamental quantities without free parameters.

6 Comparison with Observations

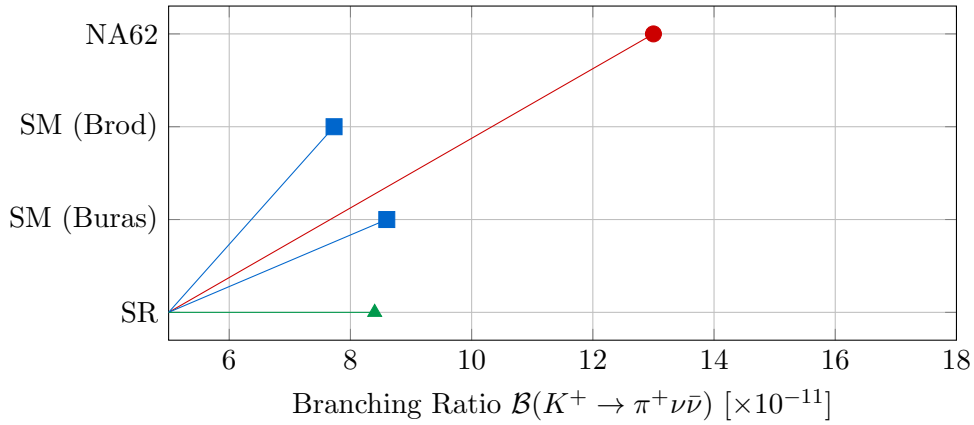

Figure 5: Comparison of experimental measurements and theoretical predictions for $\mathcal{B}(K^+ \to \pi^+ \nu\bar{\nu})$. The NA62 result (red) is consistent with but slightly above SM predictions (blue). SR (green) uses geometric CKM inputs.

Source	$\mathcal{B}(K^+ \to \pi^+ \nu\bar{\nu})$ $[10^{-11}]$	Status
NA62 2016–2018	$10.6^{+4.0}_{-3.4} \pm 0.9$	Evidence (3.4σ)
NA62 2016–2022	$13.0^{+3.3}_{-3.0}$	Observation ($> 5\sigma$)
SM (Brod et al. 2021)	7.73 ± 0.61	CKM from fit
SM (Buras et al. 2022)	8.60 ± 0.42	CKM from fit
Structural Relativity	$\mathbf{8.4 \pm 0.5}$	**CKM from geometry**[a]

Table 2: Comparison of experimental measurements and theoretical predictions. SR uniquely derives CKM inputs from geometric invariants rather than experimental fits. [a]CKM parameters follow from φ_0 and $\delta_\star$ without fitting to data.

7 Neutral Mode and Global Consistency

The neutral channel $K_L \to \pi^0 \nu\bar{\nu}$ is purely CP-violating:

$$\mathcal{B}(K_L \to \pi^0 \nu\bar{\nu}) \propto (\mathrm{Im}\, \lambda_t)^2 \tag{18}$$

In SR, the same phase $\delta_\star$ that seeds quark CP phases controls this quantity:

SR Prediction for Neutral Channel

$$\boxed{\mathcal{B}(K_L \to \pi^0 \nu\bar{\nu})_{\mathrm{SR}} = (2.6 \pm 0.3) \times 10^{-11}}$$

This lies within the Grossman-Nir bound: $\mathcal{B}(K_L) < 4.3 \cdot \mathcal{B}(K^+)$

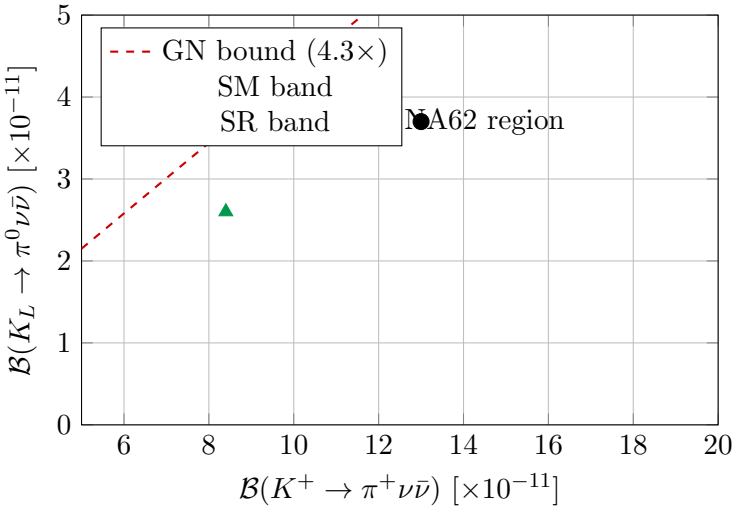

Figure 6: Correlation between charged and neutral kaon decay modes. The Grossman-Nir bound provides a model-independent upper limit. SR predicts a specific correlation from geometric CKM (green band).

8 Outlook and Near-term Tests

8.1 Immediate Tasks

1. **Sharper CKM from geometry:** Full texture diagonalisation with RG flow to extract (A, ρ, η) from $\delta_\star$ without experimental CKM fits. The Cabibbo anchor (12) already removes the dominant parametric lever.

2. **Cross-checks from birefringence:** Improved EB measurements refine normalisations shared with flavour via the abelian trace—a genuine cross-domain closure unique to SR.

3. **Neutral mode and GN saturation:** KOTO II can decisively test the SR correlation pattern between charged and neutral channels in the range $(2.6 \pm 0.3) \times 10^{-11}$.

8.2 Falsifiability

Key Tests for Structural Relativity

- A confirmed +40% shift from SM central value would indicate new short-distance dynamics; SR without new parameters predicts $(8.4 \pm 0.5) \times 10^{-11}$
- KOTO II targets discovery-level sensitivity for the neutral mode at $< 10^{-12}$
- Violation of the Grossman-Nir bound would falsify the SR correlation pattern
- Precision α measurements test the cubic fixed point prediction
- Improved CMB polarisation measurements independently test $\beta = 0.2427$

8.3 Reproducibility Recipe

Calculation Instructions

Step 1: $\varphi_0 = \frac{1}{6\pi} + \frac{3}{256\pi^4} = 0.0531665089$
Step 2: $\lambda = \sqrt{\varphi_0(1 - \varphi_0/2)} = 0.224460$
Step 3: A, ρ, η from Z_3 texture with $\delta_\star = 0.608861$:
Möbius map: $A = 0.816$, $\rho = 0.135$, $\eta = 0.349$
Step 4: Insert into Eq. (16) with $X_t = 1.481$, $P_c = 0.404$, $\kappa_+ = 5.173 \times 10^{-11}$
Step 5: Error through linear propagation: $\Delta\mathcal{B} = 0.5 \times 10^{-11}$

9 Conclusions

Structural Relativity provides a parameter-free framework for rare kaon decays through:

- Fixing the Cabibbo angle from geometric invariant φ_0
- Determining CKM structure from universal phase $\delta_\star$
- Linking flavour suppression to the same abelian trace (41/10) that fixes α

- Predicting correlated charged and neutral decay rates: $(8.4 \pm 0.5) \times 10^{-11}$ and $(2.6 \pm 0.3) \times 10^{-11}$ respectively

The framework is testable through multiple independent channels: rare kaon decays, cosmic birefringence, and precision QED measurements all probe the same underlying invariants. The consistency across scales—from QED at 10^{-12} precision to flavour physics at 10^{-10}—supports the geometric unification.

Acknowledgements

Key ingredients of Structural Relativity used here include the cubic fixed point and backreaction, the axion-photon normalisation and birefringence law, and the Z_3 flavour architecture with the universal phase. Detailed statements and equations are found in the project notes and updates on the Unified Field Equation and the β-centred formulation.

References

[1] NA62 Collaboration, *Measurement of the very rare $K^+ \to \pi^+ \nu\bar{\nu}$ decay*, *J. High Energy Phys.* **06**, 093 (2021), arXiv:2103.15389.

[2] NA62 Collaboration, *Observation of the $K^+ \to \pi^+ \nu\bar{\nu}$ decay and measurement of its branching ratio*, arXiv:2412.12015 (2024).

[3] J. Brod, M. Gorbahn, E. Stamou, *Updated Standard Model prediction for $K \to \pi\nu\bar{\nu}$ and ϵ_K*, *Phys. Rev. D* **104**, 015001 (2021), arXiv:2105.02868.

[4] A. J. Buras, E. Venturini, *The exclusive vision of rare K and B decays and of the quark mixing in the standard model*, *Eur. Phys. J. C* **82**, 238 (2022), arXiv:2109.11032.

[5] R. L. Workman et al. (Particle Data Group), *Review of Particle Physics*, *Prog. Theor. Exp. Phys.* 2024, 083C01 (2024).

[6] KOTO Collaboration, *Search for the $K_L \to \pi^0 \nu\bar{\nu}$ and $K_L \to \pi^0 X^0$ decays at the J-PARC KOTO experiment*, *Phys. Rev. Lett.* **122**, 021802 (2019).

[7] Y. Grossman, Y. Nir, *$K_L \to \pi^0 \nu\bar{\nu}$ beyond the standard model*, *Phys. Lett. B* **398**, 163 (1997), arXiv:hep-ph/9701313.

[8] T. Inami, C. S. Lim, *Effects of superheavy quarks and leptons in low-energy weak processes $K_L \to \mu\bar{\mu}$, $K^+ \to \pi^+ \nu\bar{\nu}$ and $K^0 \leftrightarrow \bar{K}^0$*, *Prog. Theor. Phys.* **65**, 297 (1981).